

## Electronic Supplementary Information

### **Establishment of different aliphatic amines-based rapid self-healing Mg(OH)<sub>2</sub> metallogels: Exploring the morphology, rheology and intriguing Semiconducting Schottky Diode characteristics**

Santanu Majumdar<sup>a</sup>, Baishakhi Pal<sup>b</sup>, Gerald Lepcha<sup>a</sup>, Krishna Sundar Das<sup>c</sup>, Indrajit Pal,<sup>a</sup> Partha Pratim Ray<sup>b,\*</sup>, Biswajit Dey<sup>a,\*</sup>

<sup>a</sup>Department of Chemistry, Visva-Bharati University, Santiniketan 731235, India.

<sup>±</sup>Department of Physics, Jadavpur University, Kolkata-700032, India.

<sup>†</sup>School of Chemical Sciences, Indian Association for the Cultivation of Science, Jadavpur, Kolkata, West Bengal 700032

#### **Corresponding Author**

\*(B.D.) E-mail: bdeychem@gmail.com

\*(P.P.R) E-mail: partha@phys.jdvu.ac.in

**1. Minimum Critical Gelation Concentration (MGC) of the synthesized (a) Mg@EN (b) Mg@TETA (c) Mg@DETA (d) Mg@TEMED and (e) Mg@TEA metallogels.**

The minimum critical gel concentrations (MGC) of Mg@EN, Mg@TETA, Mg@DETA, Mg@TEMED and Mg@TEA metallogels have been estimated. For all the amine directed metallogels, the concentrations of gel-forming chemical-ingredients i.e.  $\text{Mg}(\text{NO}_3)_2 \cdot 6\text{H}_2\text{O}$ , and various aliphatic amines were critically analyzed to determine the MGC. For all the cases metal concentration were taken from lower concentration in 1 ml water and 50% of 1 ml aqueous solution of ethylene diamine, TETA, DETA, and TEMED were taken to form the metallogels. In case of Mg@TEA 1 ml of TEA was used instead of 50% of 1 ml aqueous solution with 1 ml aqueous solution of metal salt.

The best quality gel of the Mg@EN metallogel was appeared when the concentration of  $\text{Mg}(\text{NO}_3)_2 \cdot 6\text{H}_2\text{O}$  salt and ethylenediamine (en) were taken as 1.15 mmol ( $296.6 \pm 0.1$  mg)/ml and 1 ml en solution (en:H<sub>2</sub>O = 1:1 v/v), respectively (Table S1).

**Table S1.** The concentrations of gel-forming chemicals and the serial no designated as (i), (ii), (iii), (iv) and (v) are shown in Figure S1 respectively.

Serial No	Metal Concentration (in 1 ml H <sub>2</sub> O)	Ethylenediamine (0.5 ml en taken in 0.5 ml H <sub>2</sub> O)	Phase
(i)	0.578 mmol ( $148.3 \pm 0.1$ mg) /ml	1 ml en solution	Less viscous sol
(ii)	0.694 mmol ( $177.9 \pm 0.1$ mg)/ml	1 ml en solution	Viscous sol
(iii)	0.867 mmol ( $222.4 \pm 0.1$ mg)/ml	1 ml en solution	More viscous sol
(iv)	1.041 mmol ( $266.9 \pm 0.1$ mg)/ml	1 ml en solution	More viscous sol
(v)	1.15 mmol ( $296.6 \pm 0.1$ mg)/ml	1 ml en solution	Gel

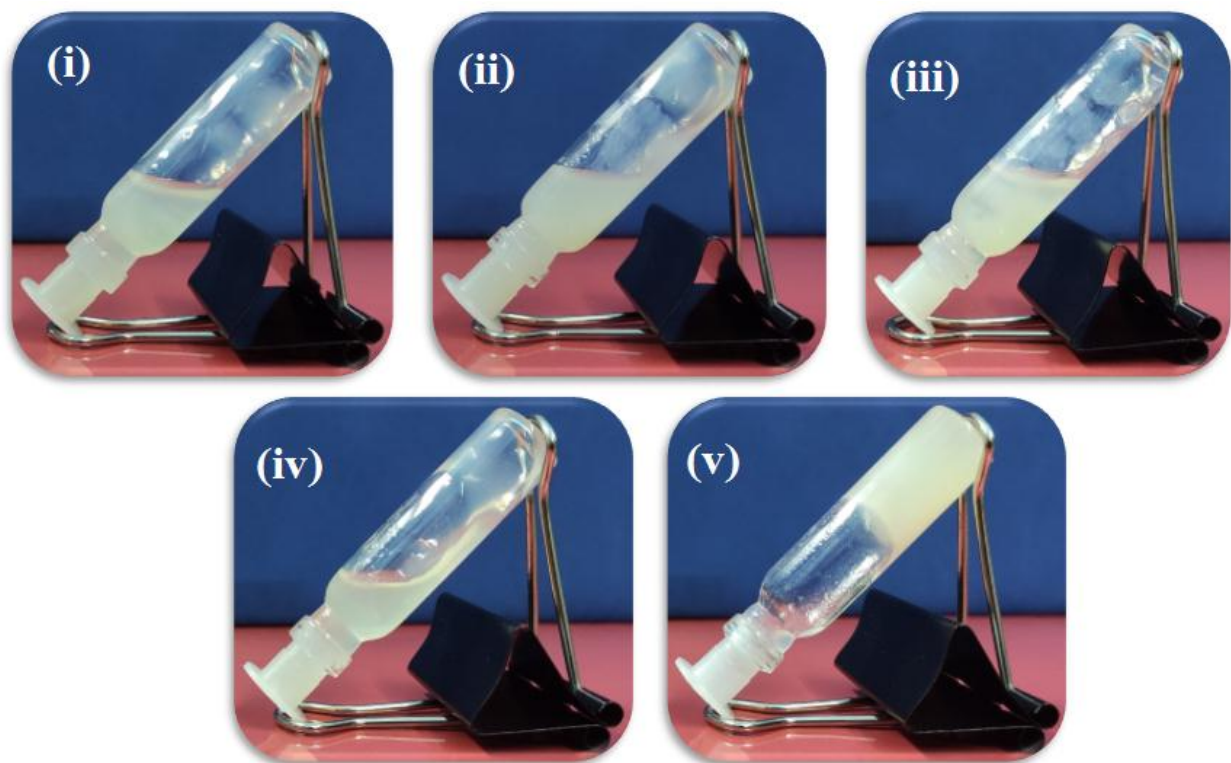


**Figure S1** Determination of Minimum Critical Gelation Concentration of the **Mg@EN** metallogel with step-wise photography of **Mg@EN** metallogel forming chemical constituents having varied concentrations.

The best quality gel of the **Mg@TETA** metallogel was appeared when the concentration of  $\text{Mg}(\text{NO}_3)_2 \cdot 6\text{H}_2\text{O}$  salt and TETA were taken as  $0.867 \text{ mmol}$  ( $222.4 \pm 0.1 \text{ mg}$ )/ml and 1 ml TETA solution (TETA: $\text{H}_2\text{O}$  = 1:1 v/v), respectively (Table S2).

**Table S2.** The concentrations of gel-forming chemicals and the serial no designated as (i), (ii), (iii), (iv) and (v) are shown in Figure S2 respectively.

Serial No	Metal Concentration (in 1 ml $\text{H}_2\text{O}$ )	TETA (0.5 ml TETA taken in 0.5 ml $\text{H}_2\text{O}$ )	Phase
(i)	$0.289 \text{ mmol}$ ( $74.1 \pm 0.1 \text{ mg}$ )/ml	1 ml TETA solution	Less viscous sol
(ii)	$0.404 \text{ mmol}$ ( $103.8 \pm 0.1 \text{ mg}$ )/ml	1 ml TETA solution	Less viscous sol
(iii)	$0.578 \text{ mmol}$ ( $148.3 \pm 0.1 \text{ mg}$ )/ml	1 ml TETA solution	More viscous sol
(iv)	$0.694 \text{ mmol}$ ( $177.9 \pm 0.1 \text{ mg}$ )/ml	1 ml TETA solution	More viscous sol
(v)	$0.867 \text{ mmol}$ ( $222.4 \pm 0.1 \text{ mg}$ )/ml	1 ml TETA solution	Gel

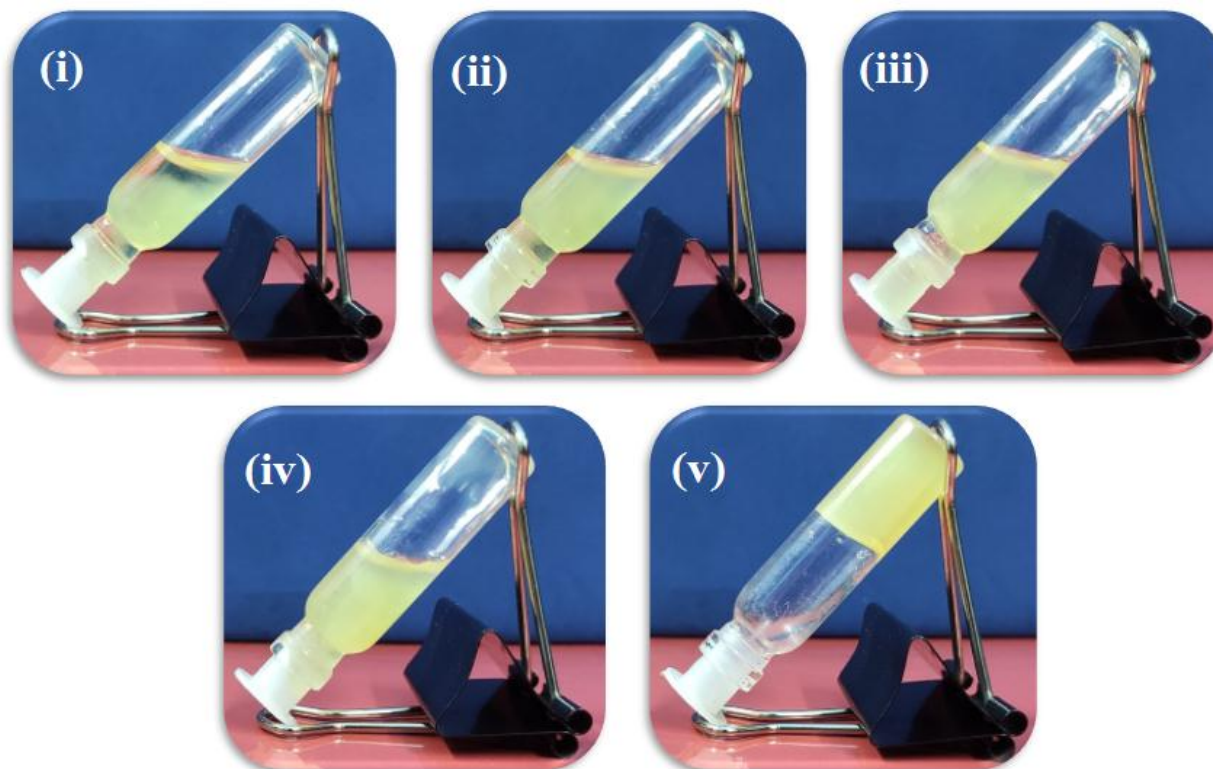


**Figure S2** Determination of Minimum Critical Gelation Concentration of the **Mg@TETA** metallogel with step-wise photography of **Mg@TETA** metallogel forming chemical constituents having varied concentrations.

The best quality gel of the Mg@DETA metallogel was appeared when the concentration of  $\text{Mg}(\text{NO}_3)_2 \cdot 6\text{H}_2\text{O}$  salt and DETA were taken as  $0.694 \text{ mmol}$  ( $177.9 \pm 0.1 \text{ mg}$ ) /ml and 1 ml DETA solution (DETA: $\text{H}_2\text{O}$  = 1:1 v/v), respectively (Table S3).

**Table S3.** The concentrations of gel-forming chemicals and the serial no designated as (i), (ii), (iii), (iv) and (v) are shown in Figure S3 respectively.

Serial No	Metal Concentration (in 1 ml $\text{H}_2\text{O}$ )	DETA (0.5 ml DETA taken in 0.5 ml $\text{H}_2\text{O}$ )	Phase
(i)	0.115 mmol ( $29.6 \pm 0.1 \text{ mg}$ )/ml	1 ml DETA solution	Less viscous sol
(ii)	0.289 mmol ( $74.1 \pm 0.1 \text{ mg}$ )/ml	1 ml DETA solution	viscous sol
(iii)	0.404 mmol ( $103.8 \pm 0.1 \text{ mg}$ )/ml	1 ml DETA solution	More viscous sol
(iv)	0.578 mmol ( $148.3 \pm 0.1 \text{ mg}$ )/ml	1 ml DETA solution	More viscous sol
(v)	0.694 mmol ( $177.9 \pm 0.1 \text{ mg}$ ) /ml	1 ml DETA solution	Gel

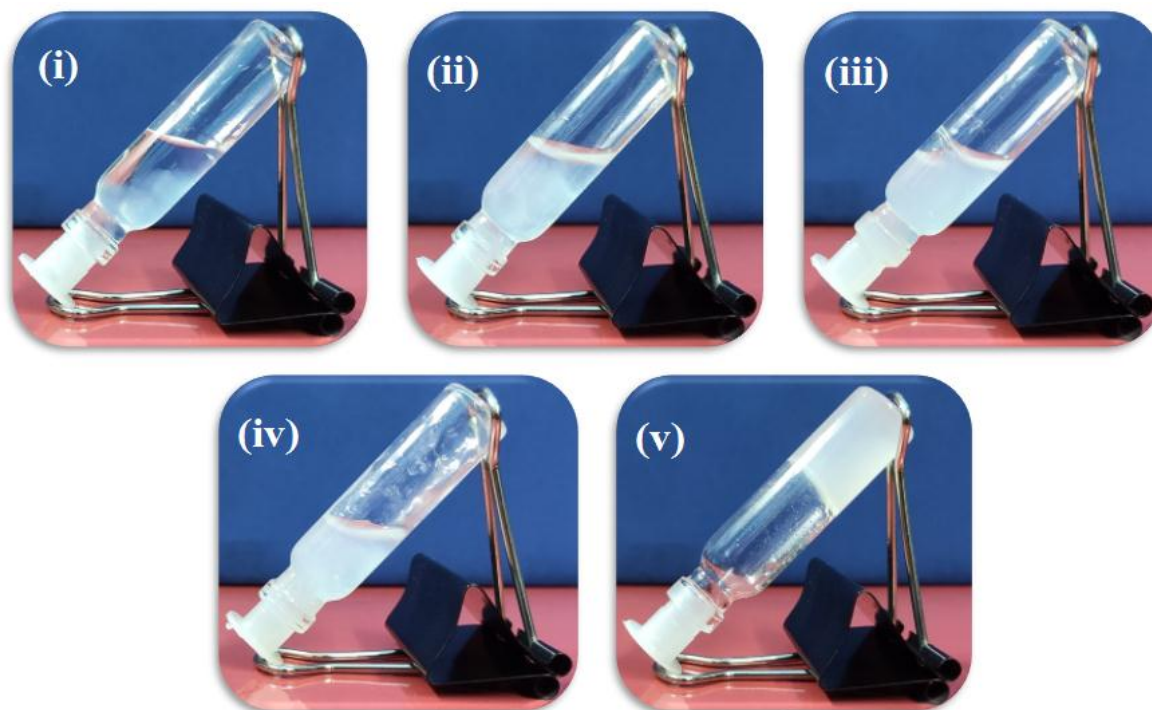


**Figure S3** Determination of Minimum Critical Gelation Concentration of the **Mg@DETA** metallogel with step-wise photography of **Mg@DETA** metallogel forming chemical constituents having varied concentrations.

The best quality gel of the **Mg@TEMED** metallogel was appeared when the concentration of  $\text{Mg}(\text{NO}_3)_2 \cdot 6\text{H}_2\text{O}$  salt and **TEMED** were taken as  $1.15 \text{ mmol}$  ( $296.6 \pm 0.1 \text{ mg}$ )/ml and 1 ml DETA solution (DETA: $\text{H}_2\text{O}$  = 1:1 v/v), respectively (Table S4).

**Table S4.** The concentrations of gel-forming chemicals and the serial no designated as (i), (ii), (iii), (iv), and (v) are shown in Figure S4 respectively.

Serial No	Metal Concentration (in 1 ml $\text{H}_2\text{O}$ )	TEMED (0.5 ml TEMED taken in 0.5 ml $\text{H}_2\text{O}$ )	Phase
(i)	0.578 mmol ( $148.3 \pm 0.1 \text{ mg}$ )/ml	1 ml TEMED solution	Less viscous sol
(ii)	0.694 mmol ( $177.9 \pm 0.1 \text{ mg}$ )/ml	1 ml TEMED solution	Viscous sol
(iii)	0.867 mmol ( $222.4 \pm 0.1 \text{ mg}$ )/ml	1 ml TEMED solution	More viscous sol
(iv)	1.012 mmol ( $259.5 \pm 0.1 \text{ mg}$ )/ml	1 ml TEMED solution	Weak gel
(v)	1.15 mmol ( $296.6 \pm 0.1 \text{ mg}$ )/ml	1 ml TEMED solution	Gel

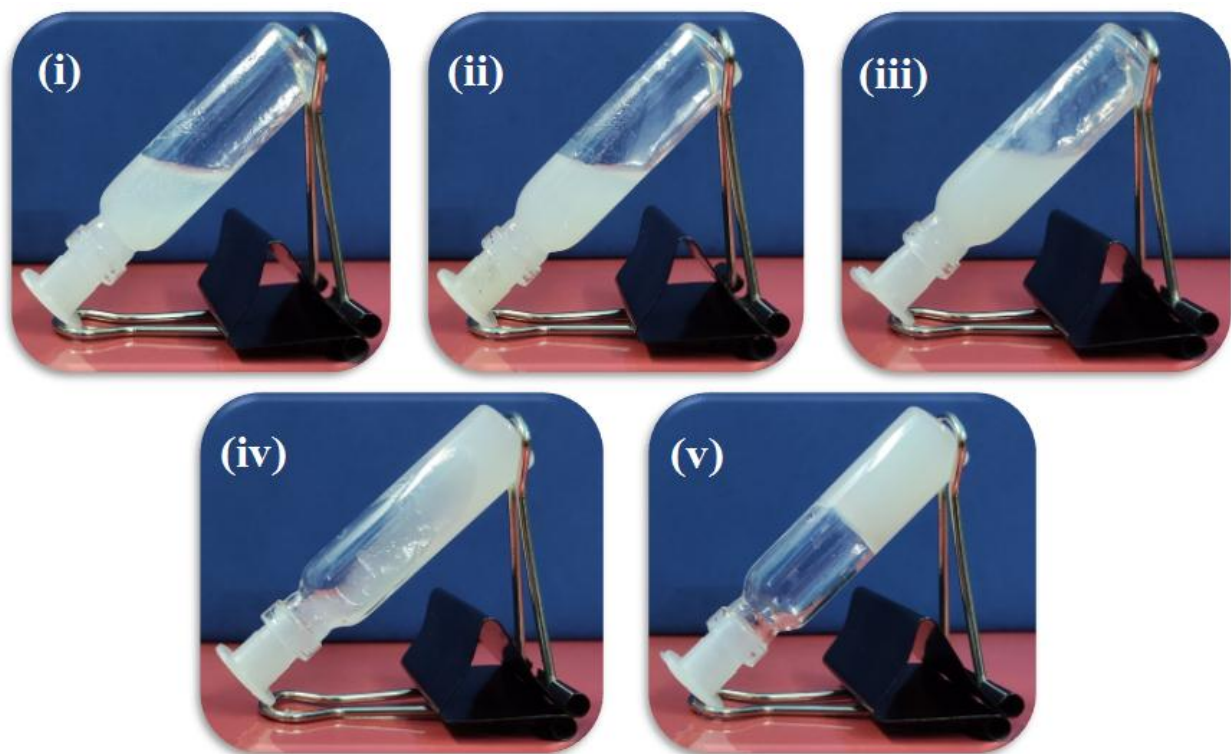


**Figure S4** Determination of Minimum Critical Gelation Concentration of the **Mg@TEMED** metallogel with step-wise photography of **Mg@TEMED** metallogel forming chemical constituents having varied concentrations.

The best quality gel of the **Mg@TEA** metallogel was appeared when the concentration of  $\text{Mg}(\text{NO}_3)_2 \cdot 6\text{H}_2\text{O}$  salt and **TEA** were taken as  $2.02 \text{ mmol}$  ( $519.0 \pm 0.1 \text{ mg}$ )/ml and  $1 \text{ ml}$  pure **TEA** respectively (Table S5).

**Table S5.** The concentrations of gel-forming chemicals and the serial no designated as (i), (ii), (iii), (iv) and (v) are shown in Figure S3 respectively.

Serial No	Metal Concentration (in 1 ml $\text{H}_2\text{O}$ )	Triethylamine	Phase
(i)	$0.867 \text{ mmol}$ ( $222.4 \pm 0.1 \text{ mg}$ )/ml	$1 \text{ ml Et}_3\text{N}$	Viscous Sol
(ii)	$1.15 \text{ mmol}$ ( $296.6 \pm 0.1 \text{ mg}$ )/ml	$1 \text{ ml Et}_3\text{N}$	Viscous sol
(iii)	$1.445 \text{ mmol}$ ( $370.7 \pm 0.1 \text{ mg}$ )/ml	$1 \text{ ml Et}_3\text{N}$	More viscous sol
(iv)	$1.735 \text{ mmol}$ ( $444.9 \pm 0.1 \text{ mg}$ )/ml	$1 \text{ ml Et}_3\text{N}$	Weak gel
(v)	$2.02 \text{ mmol}$ ( $519.0 \pm 0.1 \text{ mg}$ )/ml	$1 \text{ ml Et}_3\text{N}$	Gel

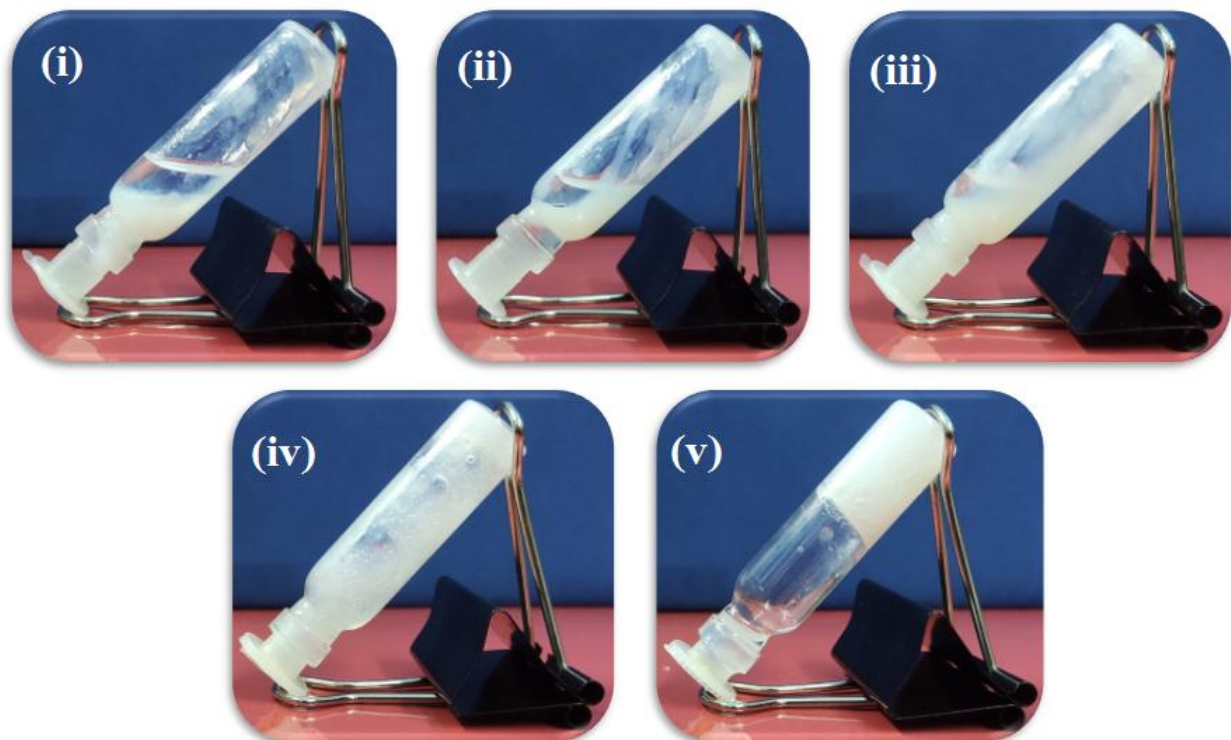


**Figure S5** Determination of Minimum Critical Gelation Concentration of the **Mg@TEA** metallo gel with step-wise photography of **Mg@TEA** metallo gel forming chemical constituents having varied concentrations.

## 2. Rheological Analysis

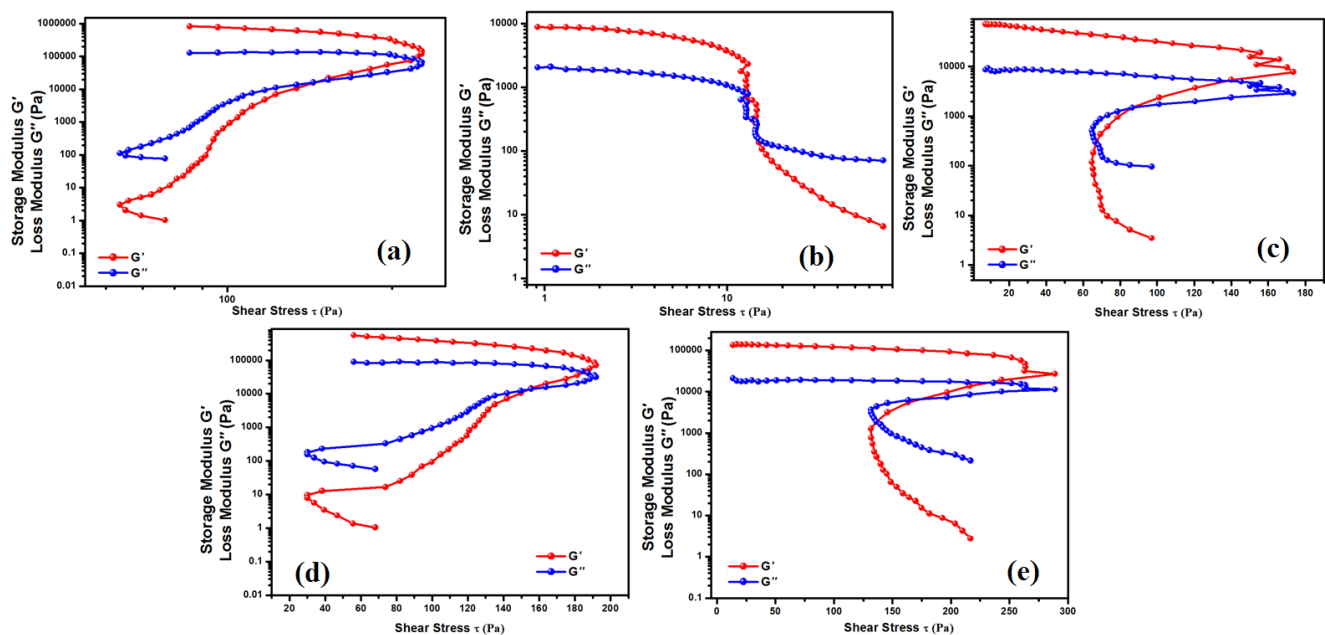


**Figure S6** Stress sweep of (a) Mg@EN, (b) Mg@TETA, (c) Mg@TEA, (d) Mg@DETA, (e) Mg@TEMED.

### **3. Visualization of Self-Healing and Load-Bearing properties of Mg@EN, Mg@TETA, Mg@TEA, Mg@DETA, Mg@TEMED metallohydrogels.**

The stability of the Mg@EN metallohydrogel against gravitational force is shown in Figure 4(a). The Mg@EN metallohydrogel was then taken out from the injection-vial and placed on a glass slide (Figure 4(b)). Then the metallohydrogel was fragmented and further this block was restored by self-healing process (Figure 4(c)). Figure 4(d) shows that the Mg@EN metallohydrogel can sustain in the tip of pin which ratifies the exceptional stability of the metallohydrogel. Figure 4(e) displays the load-bearing capability of the Mg@EN metallohydrogel and it was found that the load bearing capacity is 31.6721 ( $\pm 0.0001$ ) gm.

The stability of the Mg@TETA metallohydrogel against gravitational force is shown in Figure 5(a). The Mg@TETA metallohydrogel was then taken out from the injection-vial and placed on a glass slide (Figure 5(b)). Then the metallohydrogel was fragmented and further this block was restored by self-healing process (Figure 5(c)). Figure 5(d) shows that the Mg@TETA metallohydrogel can sustain in the tip of pin which ratifies the exceptional stability of the metallohydrogel. Figure 5(e) displays the load-bearing capability of the Mg@TETA metallohydrogel and it was found that the load bearing capacity is 36.7726 ( $\pm 0.0001$ ) gm.

The stability of the Mg@TEA metallohydrogel against gravitational force is shown in Figure 6(a). The Mg@TEA metallohydrogel was then taken out from the injection-vial and placed on a glass slide (Figure 6(b)). Then the metallohydrogel was fragmented and further this block was restored by self-healing process (Figure 6(c)). Figure 6(d) displays the load-bearing capability of the Mg@TEA metallohydrogel and it was found that the load bearing capacity is 22.1482 ( $\pm 0.0001$ ) gm.

The stability of the Mg@DETA metallohydrogel against gravitational force is shown in Figure 7(a). The Mg@DETA metallohydrogel was then taken out from the injection-vial and placed on a glass slide (Figure 7(b)). Then the metallohydrogel was fragmented and further this block was restored by self-healing process (Figure 7(c)). Figure 7(d) displays the load-bearing capability of the Mg@DETA metallohydrogel and it was found that the load bearing capacity is 16.5660 ( $\pm 0.0001$ ) gm.



The stability of the Mg@TEMED metallohydrogel against gravitational force is shown in Figure 8(a). The Mg@TEMED metallohydrogel was then taken out from the injection-vial and placed on a glass slide (Figure 8(b)). Then the metallohydrogel was fragmented and further this block was restored by self-healing process (Figure 8(c)). Figure 8(d) displays the load-bearing capability of the Mg@TEMED metallohydrogel and it was found that the load bearing capacity is 16.4825 ( $\pm 0.0001$ ) gm.

#### 4. Thermionic Emission theory:

According to Thermionic Emission theory, the forward bias current density can be expressed as

$$J = J_0 \left[ \exp\left(\frac{qV}{\eta KT}\right) - 1 \right] \quad (1)$$

$$J_0 = \text{Saturation Current Density} = A^* T^2 \exp\left(-\frac{q\Phi_B}{KT}\right) \quad (2)^1$$

Where,  $q$ =Electronic Charge,  $V$ =Applied Voltage,  $\eta$ = Ideality Factor,  $K$ =Boltzman's Constant,  $T$ =Temperature in Kelvin scale,  $\Phi_B$ = Barrier potential Height,  $A^*$ = Recharadson's constant and was considered as  $1.2 \times 10^6 \text{ A m}^{-2} \text{ K}^{-2}$ .

#### 5. Cheung's method:

According to Cheung's model, when a series resistance is designed as a series combination of resistor and diode, then the voltage across the diode can be substituted as the voltage drop across the series combination of diode and resistor. Then equation (1) can be drafted as,

$$J = J_0 \left[ \exp\left(\frac{q(V - IR_s)}{\eta KT}\right) \right] \quad (3)$$

Where,  $IR_s$  term indicates the voltage drop across the series resistance of the semiconductor diode. Inserting the value of saturation current density into equation (3), and differentiate with respect to  $\ln J$ , we get,

$$\frac{dV}{d \ln J} = A J R_s + \frac{\eta KT}{q} \quad (4)$$

Where,  $R_s$ =series resistance,  $q$ =Electronic Charge,  $\eta$ = Ideality Factor,  $K$ =Boltzman's Constant,  $T$ =Temperature in Kelvin scale

As stated in the Cheung model, the current density-reliant function  $H(J)$  can be written as,

$$H(J) = V - \frac{\eta kT}{q} \ln\left(\frac{J}{A^* T^2}\right) = A J R_S + \eta \Phi_B \quad (5)$$

Where,  $\Phi_B$  = Barrier height,  $A^*$  = Richardson's constant and was considered as  $1.2 \times 10^6 \text{ A m}^{-2} \text{ K}^{-2}$

The curve of  $dV/d\ln(J)$  vs.  $J$  in Figure S7 (a-e) is linear. The y-axis intercept of this figure yields the ideality factors ( $\eta$ ) of the SBDs. The diodes' barrier height ( $\phi_b$ ) is calculated from the y axis intercept of the  $H(J)$  vs.  $J$  linear plots shown in Figure S7 (a-e). Table S6 shows the calculated ideality factor and barrier height for the Al/Compounds junction in dark conditions. The ideality factors for Mg@TEA, Mg@DETA and Mg@TEMED based devices deviated from unity, as can be shown.

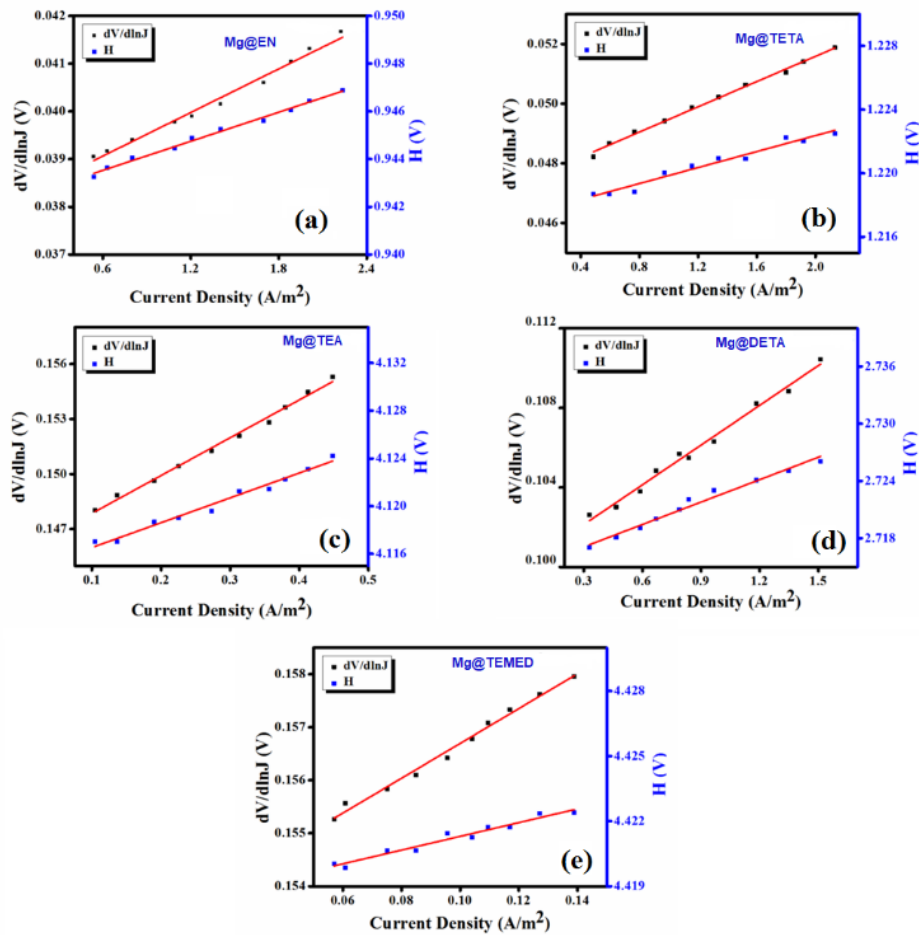


**Figure S7** Under dark conditions,  $dV/d\ln J$  vs.  $J$  and  $H(J)$  vs.  $J$  curves in double y axis for (a) Mg@EN, (b) Mg@TETA, (c) Mg@TEA, (d) Mg@DETA, (e) Mg@TEMED

Multiple generation and recombination of charge transporters in the junction section via boundary traps and inhomogeneous barrier height is the cause of the variation.<sup>2</sup> However, it should be observed that the ideality factor of the devices for Mg@EN and Mg@TETA is nearing unity. This indicates that there is less interfacial charge recombination at the junction and that Schottky junctions have superior barrier uniformity. In the dark, the calculated barrier heights for Al/Compounds junctions are 0.64 eV, 0.67 eV, 0.71 eV, 0.74 eV, 0.75 eV, for Mg@EN, Mg@TETA, Mg@DETA, Mg@TEA, and Mg@TEMED respectively. As a result of these criteria, Mg@EN emerged as a better and potential contender in terms of electrical conductivity than that of others.

**Table S6**

Sample	Series Resistance ( $\Omega$ ) from		Ideality factor ( $\eta$ )	Barrier Height $\phi_b$ (eV)
	dV/dlnJ vs. J curve	H vs. J curve		
Mg@EN	0.21 K	0.29 K	1.46	0.64
Mg@TETA	0.30 K	0.38 K	1.81	0.67
Mg@TEA	2.91 K	2.90 K	5.58	0.74
Mg@DETA	0.94 K	1.11 K	3.83	0.71
Mg@TEMED	4.65 K	4.69 K	5.87	0.75

References:

- [1] S. K. Cheung and N. W. Cheung, Extraction of Schottky diode parameters from forward current- voltage characteristics, *Appl. Phys. Lett.* 1998, **49**, 85–87.
- [2] J. Datta, M. Das, S. Sil, S. Kumar, A. Dey, R. Jana, S. Bandyopadhyay and P. P. Ray, *Mater. Sci. Semicond.*, 2019, **91**, 133-145.